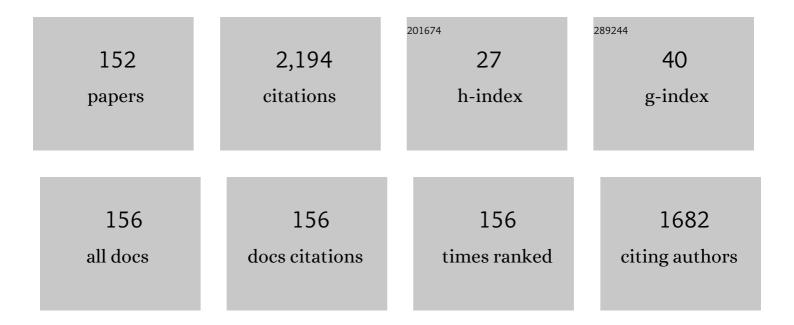
Francesco G Della Corte

List of Publications by Year in descending order

Source: https://exaly.com/author-pdf/3548142/publications.pdf Version: 2024-02-01



#	Article	IF	CITATIONS
1	Junction temperature measurement in optically-activated power MOSFET. Journal of Optics (United) Tj ETQq1	1 0.784314 2.2	rgBT /Overloo
2	Temperature dependence of the thermo-optic coefficient in 4H-SiC and GaN slabs at the wavelength of 1550Ânm. Scientific Reports, 2022, 12, 4809.	3.3	5
3	Performance Evaluation of Silicon and GaN Switches for a Small Wireless Power Transfer System. Energies, 2022, 15, 3029.	3.1	3
4	Highâ^'Performance 4Hâ^'SiC UV pâ^'iâ^'n Photodiode: Numerical Simulations and Experimental Results. Electronics (Switzerland), 2022, 11, 1839.	3.1	6
5	Near-Infrared Graphene/4H-SiC Schottky Photodetectors. , 2022, , .		Ο
6	Simulation Study of Carbon Vacancy Trapping Effect on Low Power 4H-SiC MOSFET Performance. Silicon, 2021, 13, 3629-3637.	3.3	7
7	Study and Assessment of Defect and Trap Effects on the Current Capabilities of a 4H-SiC-Based Power MOSFET. Electronics (Switzerland), 2021, 10, 735.	3.1	3
8	A Technique for the Direct Measurement of the Junction Temperature in Power Light Emitting Diodes. IEEE Sensors Journal, 2021, 21, 6293-6299.	4.7	4
9	A Technique for Improving the Precision of the Direct Measurement of Junction Temperature in Power Light-Emitting Diodes. Sensors, 2021, 21, 3113.	3.8	5
10	Acoustic Simulation for Performance Evaluation of Ultrasonic Ranging Systems. Electronics (Switzerland), 2021, 10, 1298.	3.1	6
11	Ranging with Frequency Dependent Ultrasound Air Attenuation. Sensors, 2021, 21, 4963.	3.8	3
12	Exploiting RFID technology for Indoor Positioning. , 2021, , .		4
13	An Efficient 4H-SiC Photodiode for UV Sensing Applications. Electronics (Switzerland), 2021, 10, 2517.	3.1	8
14	Ultrasonic Ranging using Frequency Selective Attenuation. , 2021, , .		0
15	Tiny Machine Learning Techniques for Driving Behavior Scoring in a Connected Car Environment. , 2021, , .		2
16	Analysis of the Electrical Characteristics of Mo/4H-SiC Schottky Barrier Diodes for Temperature-Sensing Applications. Journal of Electronic Materials, 2020, 49, 1322-1329.	2.2	10
17	Analysis of 4H-SiC MOSFET with distinct high-k/4H-SiC interfaces under high temperature and carrier-trapping conditions. Applied Physics A: Materials Science and Processing, 2020, 126, 1.	2.3	7
18	Simulation and analysis of the forward bias current–voltage–temperature characteristics of W/4H-SiC Schottky barrier diodes for temperature-sensing applications. Solid State Electronics Letters, 2020, 2, 49-54.	1.0	3

#	Article	IF	CITATIONS
19	LED junction temperature prediction using machine learning techniques. , 2020, , .		5
20	Enhanced Non-Uniformity Modeling of 4H-SiC Schottky Diode Characteristics Over Wide High Temperature and Forward Bias Ranges. IEEE Journal of the Electron Devices Society, 2020, 8, 1339-1344.	2.1	7
21	Simulating Signal Aberration and Ranging Error for Ultrasonic Indoor Positioning. Sensors, 2020, 20, 3548.	3.8	15
22	Mobile Synchronization Recovery for Ultrasonic Indoor Positioning. Sensors, 2020, 20, 702.	3.8	28
23	Temperature Sensing Characteristics and Long Term Stability of Power LEDs Used for Voltage vs. Junction Temperature Measurements and Related Procedure. IEEE Access, 2020, 8, 43057-43066.	4.2	12
24	Augmented Information Discovery using NFC Technology within a Platform for Disaster Monitoring. , 2020, , .		0
25	Indoor Object Positioning using Smartphone and RFID or QRCode. , 2020, , .		3
26	Power LED junction temperature readout circuit based on an off-the-shelf LED driver. , 2020, , .		0
27	Power MOSFET Intrinsic Diode as a Highly Linear Junction Temperature Sensor. IEEE Sensors Journal, 2019, 19, 11034-11040.	4.7	4
28	Electronic sensors for intraoral force monitoring: state-of-the-art and comparison. Procedia CIRP, 2019, 79, 730-733.	1.9	3
29	Multiobjective Optimization of Design of 4H-SiC Power MOSFETs for Specific Applications. Journal of Electronic Materials, 2019, 48, 3871-3880.	2.2	30
30	Temperature and SiO2/4H-SiC interface trap effects on the electrical characteristics of low breakdown voltage MOSFETs. Applied Physics A: Materials Science and Processing, 2019, 125, 1.	2.3	30
31	Analytical Modeling of Dual-Junction Tandem Solar Cells Based on an InGaP/GaAs Heterojunction Stacked on a Ge Substrate. Journal of Electronic Materials, 2019, 48, 4107-4116.	2.2	17
32	Analysis of Al ₂ O ₃ high-k gate dielectric effect on the electrical characteristics of a 4H-SiC low-power MOSFET. , 2019, , .		5
33	Impact of a non-uniform p-base doping concentration on the electrical characteristics of a low power MOSFET in 4H-SiC. , 2019, , .		3
34	Simple and Low-Cost Photovoltaic Module Emulator. Electronics (Switzerland), 2019, 8, 1445.	3.1	26
35	A Real-Time Decision Platform for the Management of Structures and Infrastructures. Electronics (Switzerland), 2019, 8, 1180.	3.1	30
36	Analysis of the current-voltage-temperature characteristics of Wl4H-SiC Schottky barrier diodes for high performance temperature sensors. , 2019, , .		5

3

FRANCESCO G DELLA CORTE

#	Article	IF	CITATIONS
37	Effects of the Temperature on the Efficiency Degradation in Multi-stage RF Energy Harvesters. , 2019, , .		1
38	CMOS RF Transmitters with On-Chip Antenna for Passive RFID and IoT Nodes. Electronics (Switzerland), 2019, 8, 1448.	3.1	14
39	Reconfigurable UHF RFID tag with sensing capabilities. , 2019, , .		4
40	Open-Source Hardware Platforms for Smart Converters with Cloud Connectivity. Electronics (Switzerland), 2019, 8, 367.	3.1	19
41	An Indoor Ultrasonic System for Autonomous 3-D Positioning. IEEE Transactions on Instrumentation and Measurement, 2019, 68, 2507-2518.	4.7	53
42	Simulation and analysis of the current–voltage–temperature characteristics of Al/Ti/4H-SiC Schottky barrier diodes. Japanese Journal of Applied Physics, 2019, 58, 014002.	1.5	29
43	V ₂ O ₅ /4H-SiC Schottky Diode Temperature Sensor: Experiments and Model. IEEE Transactions on Electron Devices, 2018, 65, 687-694.	3.0	15
44	Ranging RFID Tags With Ultrasound. IEEE Sensors Journal, 2018, 18, 2967-2975.	4.7	38
45	Electro-Optical Modulation in a 4H-SiC Slab Induced by Carrier Depletion in a Schottky Diode. IEEE Photonics Technology Letters, 2018, 30, 877-880.	2.5	7
46	A V2O5/4H-SiC Schottky diode-based PTAT sensor operating in a wide range of bias currents. Sensors and Actuators A: Physical, 2018, 269, 171-174.	4.1	11
47	Interface Trap Effects in the Design of a 4H-SiC MOSFET for Low Voltage Applications. , 2018, , .		8
48	Temperature Effects on the Efficiency of Dickson Charge Pumps for Radio Frequency Energy Harvesting. IEEE Access, 2018, 6, 65729-65736.	4.2	20
49	A Direct Junction Temperature Measurement Technique for Power LEDs. , 2018, , .		4
50	Analysis of Trapping Effects on the Forward Current–Voltage Characteristics of Al-Implanted 4H-SiC p-i-n Diodes. IEEE Transactions on Electron Devices, 2018, 65, 3371-3378.	3.0	37
51	Numerical Simulation Study of a Low Breakdown Voltage 4H-SiC MOSFET for Photovoltaic Module-Level Applications. IEEE Transactions on Electron Devices, 2018, 65, 3352-3360.	3.0	34
52	A Monolithic Multisensor Microchip with Complete On-Chip RF Front-End. Sensors, 2018, 18, 110.	3.8	18
53	Analysis of the Forward l–V Characteristics of Al-Implanted 4H-SiC p-i-n Diodes with Modeling of Recombination and Trapping Effects Due to Intrinsic and Doping-Induced Defect States. Journal of Electronic Materials, 2018, 47, 1414-1420.	2.2	29
54	Energy savings in transportation: Setting up an innovative SHM method. Mathematical Modelling of Engineering Problems, 2018, 5, 323-330.	0.5	13

FRANCESCO G DELLA CORTE

#	Article	IF	CITATIONS
55	A Calorimetry Based System for Measuring the Power Losses of Switching Power Devices. Lecture Notes in Electrical Engineering, 2018, , 111-116.	0.4	0
56	RF-Powered HF-RFID Analog Sensors Platform. Lecture Notes in Electrical Engineering, 2017, , 85-91.	0.4	1
57	Numerical simulations of the electrical transport characteristics of a Pt/n-GaN Schottky diode. Japanese Journal of Applied Physics, 2017, 56, 094301.	1.5	30
58	Instrumented infrastructures for damage detection and management. , 2017, , .		19
59	Using ANT Communications for Node Synchronization and Timing in a Wireless Ultrasonic Ranging System. , 2017, 1, 1-4.		8
60	Integrated Amorphous Silicon p-i-n Temperature Sensor for CMOS Photonics. Sensors, 2016, 16, 67.	3.8	13
61	A PTAT-based Heat-flux Sensor for the Measurement of Power Losses through a Calorimetric Apparatus. Procedia Engineering, 2016, 168, 1617-1620.	1.2	2
62	85–440 K Temperature Sensor Based on a 4H-SiC Schottky Diode. IEEE Sensors Journal, 2016, 16, 6537-6542.	4.7	40
63	SPICE modelling and experiments on a complete photovoltaic system including cells, storage elements, inverter and load. , 2016, , .		2
64	A calorimetry-based measurement apparatus for switching losses in high power electronic devices. , 2016, , .		6
65	4H-SiC p-i-n diode as Highly Linear Temperature Sensor. IEEE Transactions on Electron Devices, 2016, 63, 414-418.	3.0	47
66	High-Performance Temperature Sensor Based on 4H-SiC Schottky Diodes. IEEE Electron Device Letters, 2015, 36, 720-722.	3.9	69
67	A CMOS IC for the real-time and wireless diagnostics of high concentration solar cells. , 2015, , .		0
68	Design and implementation of high resolution, high linearity temperature sensor in CMOS process. , 2015, , .		1
69	Autonomous RFID sensor platform with highly efficient energy harvesting circuit. , 2015, , .		2
70	RF-powered UHF-RFID analog sensors platform. , 2015, , .		1
71	Highly Linear Temperature Sensor Based on 4H-Silicon Carbide p-i-n Diodes. IEEE Electron Device Letters, 2015, 36, 1205-1208.	3.9	28
72	A measurement apparatus for switching losses based on an heat-flux sensor. , 2015, , .		0

#	Article	IF	CITATIONS
73	Performance assessment of an enhanced RFID sensor tag for long-run sensing applications. , 2014, , .		13
74	An autonomous and energy efficient Smart Sensor Platform. , 2014, , .		11
75	Dynamic impedance matching network for RF energy harvesting systems. , 2014, , .		18
76	SPICE modelling of a complete photovoltaic system including modules, energy storage elements and a multilevel inverter. Solar Energy, 2014, 107, 338-350.	6.1	18
77	Numerical Analysis of Electro-Optical Modulators Based on the Amorphous Silicon Technology. Journal of Lightwave Technology, 2014, 32, 2399-2407.	4.6	7
78	Progress towards a high-performing a-Si:H-based electro-optic modulator. Journal of Optics (United) Tj ETQq0 0	0 rgBT /O	verlock 10 Tf 5
79	Heat flux sensor for power loss measurements of switching devices. , 2013, , .		6
80	Use of Amorphous Silicon for Active Photonic Devices. IEEE Transactions on Electron Devices, 2013, 60, 1495-1505.	3.0	36
81	Hydrogenated amorphous silicon multi-SOI waveguide modulator with low voltage–length product. Optics and Laser Technology, 2013, 45, 204-208.	4.6	8
82	Steady-State Analysis of a Normally-Off 4H-SiC Trench Bipolar-Mode FET. Materials Science Forum, 2013, 740-742, 942-945.	0.3	5
83	Electro-optical effect in hydrogenated amorphous silicon-based waveguide-integrated p-i-p and p-i-n configurations. Optical Engineering, 2013, 52, 087110.	1.0	8
84	Static and transient analysis of a 4H-SiC trench Bipolar Mode FET with normally-off characteristics. , 2012, , .		4
85	A 25 ns switching time MachÂZehnder modulator in as-deposited a-Si:H. Optics Express, 2012, 20, 9351.	3.4	22
86	An Analytical Model of the Switching Behavior of 4H-SiC p\$^{m +}\$ -n-n\$^{m +}\$ Diodes from Arbitrary Injection Conditions. IEEE Transactions on Power Electronics, 2012, 27, 1641-1652.	7.9	25
87	Battery-less smart RFID tag with sensor capabilities. , 2012, , .		14
88	CMOS-compatible electro-optical Mach-Zehnder modulator based on the amorphous silicon technology. , 2012, , .		0
89	DESIGN CONSIDERATIONS FOR RADIO FREQUENCY ENERGY HARVESTING DEVICES. Progress in Electromagnetics Research B, 2012, 45, 19-35.	1.0	53
90	1.55 μm silicon-based reflection-type waveguide-integrated thermo-optic 2 × 2 switch. Optik, 2012, 123, 467-469.	2.9	3

FRANCESCO G DELLA CORTE

#	Article	IF	CITATIONS
91	Amorphous silicon waveguides grown by PECVD on an Indium Tin Oxide buried contact. Optics Communications, 2012, 285, 3088-3092.	2.1	8
92	Characterization of an electrically induced refractive index change in a hydrogenated amorphous silicon multistack waveguide. , 2011, , .		1
93	An Analytical Model of the Forward l– V Characteristics of 4H-SiC p-i-n Diodes Valid for a Wide Range of Temperature and Current. IEEE Transactions on Power Electronics, 2011, 26, 2835-2843.	7.9	42
94	Electro-optical modulation at 1550 nm in an as-deposited hydrogenated amorphous silicon p-i-n waveguiding device. Optics Express, 2011, 19, 2941.	3.4	33
95	Electro-Optical Modulating Multistack Device Based on the CMOS-Compatible Technology of Amorphous Silicon. Lecture Notes in Electrical Engineering, 2011, , 285-289.	0.4	Ο
96	HELIOS: photonics electronics functional integration on CMOS. Proceedings of SPIE, 2010, , .	0.8	3
97	Electrooptical Modulating Device Based on a CMOS-Compatible <formula formulatype="inline"> <tex notation="TeX">\${m alpha}\$</tex> </formula> -Si:H/ <formula formulatype="inline"> <tex notation="TeX">\${m alpha}\$</tex> -SiCN Multistack Waveguide, IEEE Journal of Selected Topics in Quantum Electronics, 2010, 16, 173-178.</formula 	2.9	16
98	CMOS wireless temperature sensor with integrated radiating element. Sensors and Actuators A: Physical, 2010, 158, 169-175.	4.1	11
99	2.6 GHz receiver for on-chip optical networking in 65nm CMOS technology. , 2010, , .		Ο
100	Low-power CMOS fully integrated transmitters exploiting on-chip antennas. , 2010, , .		1
101	CMOS fully integrated 2.5GHz active RFID tag with on-chip antenna. , 2010, , .		3
102	Wireless temperature sensor integrated circuits with on-chip antennas. , 2010, , .		2
103	Design and modeling of a novel 4H-SiC normally-off BMFET transistor for power applications. , 2010, , .		8
104	A self-consistent model of the static and switching behaviour of 4H-SiC diodes. , 2010, , .		7
105	Electro-optical modulation and photoinduced absorption effects on a CMOS-compatible $\hat{l}\pm$ -Si:H/ $\hat{l}\pm$ -SiCN multistack waveguide. , 2010, , .		Ο
106	Amorphous silicon waveguides grown by PECVD on an Indium Tin Oxide buried contact. , 2010, , .		0
107	Modulation speed improvement in a Fabry–Perot thermo-optical modulator through a driving signal optimization technique. Optical Engineering, 2009, 48, 074601.	1.0	4
108	A microchip integrated temperature sensor with RF communication channel and on-chip antenna. Procedia Chemistry, 2009, 1, 473-476.	0.7	2

Francesco G Della Corte

#	Article	IF	CITATIONS
109	On-Chip Integrated Antenna Structures for Biomedical Implantable Sensors. Procedia Chemistry, 2009, 1, 513-516.	0.7	3
110	Numerical simulations of Al implanted 4H-SiC diodes modeling an explicit carrier trap effect due to the non-substitutional Al doping concentration. , 2009, , .		2
111	Analytical model for the forward current of Al implanted 4H-SiC p-i-n diodes in a wide range of temperatures. , 2009, , .		7
112	Measurement of the IR absorption induced by visible radiation in amorphous silicon and silicon carbide thin films by an in-guide technique. Optical Materials, 2008, 30, 1240-1243.	3.6	3
113	Experimental characterization and numerical analysis of the 4H-SiC p–i–n diodes static and transient behaviour. Microelectronics Journal, 2008, 39, 1594-1599.	2.0	23
114	Electro-optically induced absorption in α-Si:H/α-SiCN waveguiding multistacks. Optics Express, 2008, 16, 7540.	3.4	32
115	A parametric study of laser induced ablation–oxidation on porous silicon surfaces. Journal of Physics Condensed Matter, 2008, 20, 265009.	1.8	12
116	Photoinduced absorption in B-doped hydrogenated amorphous silicon alloys applied to all-optical modulators. Journal of Applied Physics, 2008, 103, 023107.	2.5	5
117	Design, fabrication, and characterization of an $\hat{I}\pm$ -Si:H/ $\hat{I}\pm$ -SiCN multistack waveguide for electro optical modulation. , 2008, , .		Ο
118	Li batteries with porous sol–gel cathodes. Microelectronics Journal, 2007, 38, 637-641.	2.0	2
119	Bistable hybrids in sol–gel technology for switching devices. Microelectronics Journal, 2007, 38, 1169-1174.	2.0	1
120	Simulation and experimental results on the forward J–V characteristic of Al implanted 4H–SiC p–i–n diodes. Microelectronics Journal, 2007, 38, 1273-1279.	2.0	25
121	An integrated hybrid optical device for sensing applications. Physica Status Solidi C: Current Topics in Solid State Physics, 2007, 4, 1946-1950.	0.8	4
122	An integrated pressure-driven microsystem based on porous silicon for optical monitoring of gaseous and liquid substances. Physica Status Solidi (A) Applications and Materials Science, 2007, 204, 1459-1463.	1.8	17
123	Fabrication of Porous Sol-Gel Cathodes for Li Batteries. , 2006, , .		Ο
124	Optical Interconnects for Network on Chip. , 2006, , .		4
125	Study of in-gap defects in intrinsic and B-doped a-Si1â^'xCx:H by photo-induced optical absorption and photoluminescence. Journal of Non-Crystalline Solids, 2006, 352, 2647-2651.	3.1	1
126	A Microsystem Based on Porous Silicon-Glass Anodic Bonding for Gas and Liquid Optical Sensing. Sensors, 2006, 6, 680-687.	3.8	35

2

#	Article	IF	CITATIONS
127	In-guide pump and probe characterization of photoinduced absorption in hydrogenated amorphous silicon thin films. Journal of Applied Physics, 2006, 100, 033104.	2.5	9
128	All-optical modulation in thin film silicon-based waveguiding structures. , 2005, , .		0
129	Temperature dependence of the thermo-optic coefficient of lithium niobate, from 300 to 515 K in the visible and infrared regions. Journal of Applied Physics, 2005, 98, 036101.	2.5	64
130	1.55 - \hat{A} ím reflection-type optical waveguide switch based on thermo-optic effect. , 2003, , .		0
131	<inline-formula><math <br="" display="inline">overflow="scroll"><mn>1</mn><mo>.</mo><mn>5</mn><mo>.</mo><mi>μ</mi><mstylemathvariant="normal"><mtext>m</mtext></mstylemathvariant="normal"></math></inline-formula> silicon-based reflection-type waveguide-integrated thermo-optic switch. Optical Engineering. 2003. 42. 2835.	1.0	10
132	Design and simulation of an a-Si:H/GaAs HBT with improved DC and high-frequency characteristics. , 2003, , .		0
133	Digital optical switch based on amorphous silicon waveguide. , 2003, 5117, 581.		0
134	Digital optical switch based on amorphous silicon waveguide. , 2003, , .		2
135	Amorphous silicon thin film for all-optical micromodulator. , 2003, , .		0
136	Thermo-optic design for microwave and millimeter-wave electromagnetic power microsensors. Applied Optics, 2002, 41, 3601.	2.1	4
137	Study of the thermo-optic effect in hydrogenated amorphous silicon and hydrogenated amorphous silicon carbide between 300 and 500 K at 1.55 μm. Applied Physics Letters, 2001, 79, 168-170.	3.3	43
138	Simulation study of the DC and AC characteristics of an a-Si:H(n)/GaAs(p)/GaAs(n) heterojunction bipolar transistor. Solid-State Electronics, 2000, 44, 2265-2271.	1.4	2
139	Temperature dependence of the thermo-optic coefficient of InP, GaAs, and SiC from room temperature to 600 K at the wavelength of 1.5 μm. Applied Physics Letters, 2000, 77, 1614-1616.	3.3	109
140	Temperature dependence analysis of the thermo-optic effect in silicon by single and double oscillator models. Journal of Applied Physics, 2000, 88, 7115-7119.	2.5	89
141	Temperature dependence of the thermo-optic coefficient in crystalline silicon between room temperature and 550 K at the wavelength of 1523 nm. Applied Physics Letters, 1999, 74, 3338-3340.	3.3	179
142	Thermo-optic effect exploitation in silicon microstructures. Sensors and Actuators A: Physical, 1998, 71, 19-26.	4.1	39
143	Amorphous silicon waveguides and interferometers for low-cost silicon optoelectronics. , 1998, 3278, 286.		3

Silicon-on-insulator guided-wave structures for thermo-optic switching applications. , 1997, 3007, 22.

#	Article	IF	CITATIONS
145	<title>Silicon thermo-optic micromodulators for low-cost low-performance fiber-in-the-loop
applications</title> . , 1997, , .		0
146	Amorphous silicon waveguides and light modulators for integrated photonics realized by low-temperature plasma-enhanced chemical-vapor deposition. Optics Letters, 1996, 21, 2002.	3.3	65
147	New possibilities for efficient silicon integrated electro-optical modulators. Optics Communications, 1991, 86, 228-235.	2.1	27
148	Electro-optically induced absorption in \$alpha\$-Si:H/\$alpha\$-SiCN waveguiding multistacks. Journal of the European Optical Society-Rapid Publications, 0, 5, .	1.9	6
149	Electro-optical modulating multistack device based on the CMOS-compatible technology of amorphous silicon. Journal of the European Optical Society-Rapid Publications, 0, 5, .	1.9	1
150	Low-loss amorphous silicon waveguides grown by PECVD on indium tin oxide. Journal of the European Optical Society-Rapid Publications, 0, 5, .	1.9	12
151	Numerical Simulations of a 4H-SiC BMFET Power Transistor with Normally-Off Characteristics. Materials Science Forum, 0, 679-680, 621-624.	0.3	19
152	All-optical modulation in a CMOS-compatible amorphous silicon-based device. Journal of the European Optical Society-Rapid Publications, 0, 7, .	1.9	11